J|A|C|S ARTICLES

Published on Web 02/05/2010

2D IR Line Shapes Probe Ovispirin Peptide Conformation and Depth in Lipid Bilayers

Ann Marie Woys,[†] Yu-Shan Lin,[†] Allam S. Reddy,[‡] Wei Xiong,[†] Juan J. de Pablo,[‡] James L. Skinner,[†] and Martin T. Zanni*,[†]

Department of Chemistry, University of Wisconsin, 1101 University Avenue, Madison, Wisconsin 53706, and Department of Chemical Engineering, University of Wisconsin, Madison, Wisconsin 53706-1691

Received December 7, 2009; E-mail: woys@wisc.edu; zanni@chem.wisc.edu

Abstract: We report a structural study on the membrane binding of ovispirin using 2D IR line shape analysis, isotope labeling, and molecular dynamics simulations. Ovispirin is an antibiotic polypeptide that binds to the surfaces of membranes as an α-helix. By resolving individual backbone vibrational modes (amide I) using 1-$^{13}C{=}^{18}O$ labeling, we measured the 2D IR line shapes for 15 of the 18 residues in this peptide. A comparison of the line shapes reveals an oscillation in the inhomogeneous line width that has a period equal to that of an α-helix (3.6 amino acids). The periodic trend is caused by the asymmetric environment of the membrane bilayer that exposes one face of the α-helix to much stronger environmental electrostatic forces than the other. We compare our experimental results to 2D IR line shapes calculated using the lowest free energy structure identified from molecular dynamics simulations. These simulations predict a periodic trend similar to the experiment and lead us to conclude that ovispirin lies in the membrane just below the headgroups, is tilted, and may be kinked. Besides providing insight into the antibiotic mechanism of ovispirin, our procedure provides an infrared method for studying peptide and protein structures that relies on the natural vibrational modes of the backbone. It is a complementary method to other techniques that utilize line shapes, such as fluorescence, NMR, and ESR spectroscopies, because it does not require mutations, the spectra can be quantitatively simulated using molecular dynamics, and the technique can be applied to difficult-to-study systems like ion channels, aggregated proteins, and kinetically evolving systems.

Introduction

Protein structure and dynamics are often studied using line shape analysis of spectra from native and non-native probes. Spectroscopic line shapes show signatures of relaxation processes that transfer energy away from the spectroscopic observable (e.g., population transfer) and dephasing that is a result of structural fluctuations of the environment surrounding the observable.[1−3] Fluorescence, electron spin resonance (ESR), nuclear magnetic relaxation (NMR), and other spectroscopies use these processes to study protein structures,[4−15] although each method relies on distinct relaxation and dephasing processes. For example, ESR line widths are determined by the collision frequency of non-natural nitroxide spin labels with paramagnetic reagents that are added to the solution, and thus are proportional to solvent accessibility, among other factors.[6,8,12] By synthesizing a series of nitroxide mutants, secondary structures are identified by the measured line widths. For example, this approach has been utilized with much success to identify α-helices, which display an oscillatory trend in the ESR line widths with a period of 3.6 amino acids.[8] Much work has gone into making ESR and these other approaches viable, and now that the mechanisms of energy transfer and dephasing are understood, these methods provide an established and powerful set of tools for studying protein structures, especially those bound to membranes.

This Article reports that the natural infrared line widths of peptide and protein backbones can be used to probe structure

[†] Department of Chemistry.
[‡] Department of Chemical Engineering.

(1) Kubo, R. *Adv. Chem. Phys.* **1969**, *15*, 101–127.
(2) Berne, B. J.; Pecora, R. *Dynamic Light Scattering: With Applications to Chemistry, Biology, and Physics*; Wiley: New York, 1976.
(3) Ernst, R. R.; Bodenhausen, G.; Wokaun, A. *Principles of Nuclear Magnetic Resonance in One and Two Dimensions*; Oxford University Press: New York, 1991.
(4) Chung, L. A.; Lear, J. D.; Degrado, W. F. *Biochemistry* **1992**, *31*, 6608–6616.
(5) Johnson, J. E.; Cornell, R. B. *Biochemistry* **1994**, *33*, 4327–4335.
(6) Hubbell, W. L.; Altenbach, C. *Curr. Opin. Struct. Biol.* **1994**, *4*, 566–573.
(7) Mishra, V. K.; Palgunachari, M. N. *Biochemistry* **1996**, *35*, 11210–11220.
(8) Hubbell, W. L.; Gross, A.; Langen, R.; Lietzow, M. A. *Curr. Opin. Struct. Biol.* **1998**, *8*, 649–656.
(9) Hristova, K.; Dempsey, C. E.; White, S. H. *Biophys. J.* **2001**, *80*, 801–811.
(10) London, E.; Ladokhin, A. S. *Curr. Top. Membr.* **2002**, *52*, 89–115.
(11) Nielsen, R. D.; Che, K. P.; Gelb, M. H.; Robinson, B. H. *J. Am. Chem. Soc.* **2005**, *127*, 6430–6442.
(12) Fanucci, G. E.; Cafiso, D. S. *Curr. Opin. Struct. Biol.* **2006**, *16*, 644–653.
(13) McDermott, A. *Annu. Rev. Biophys.* **2009**, *38*, 385–403.
(14) Orioni, B.; Bocchinfuso, G.; Kim, J. Y.; Palleschi, A.; Grande, G.; Bobone, S.; Park, Y.; Kim, J. I.; Hahm, K. S.; Stella, L. *Biochim. Biophys. Acta: Biomembranes* **2009**, *1788*, 1523–1533.
(15) Franzmann, M.; Otzen, D.; Wimmer, R. *ChemBioChem* **2009**, *10*, 2339–2347.

 10.1021/ja9101776

like those other techniques, but are sensitive to a unique set of environmental forces and dynamical time scales. Infrared line widths measure dynamics on the femtosecond to few picosecond time scale, during which time the only dynamical processes come from hydrogen-bond motions and small fluctuations in the side chain and backbone structure. Dynamics like these are of interest at the active site of proteins,[16−18] for example, but it is not immediately apparent how IR line widths could be used to probe protein secondary and tertiary structures. However, we and others have found that the inhomogeneous line width of the amide I band (i.e., the carbonyl stretch of the backbone) is a good structure indicator, because it measures the amount of structural disorder of the backbone and surrounding electrostatic environment that is not averaged out after a few picoseconds.[6,8,12,19−26] Thus, disorder that appears homogeneous in ESR (or other) measurements still contributes to the inhomogeneous infrared line width. Thus, this IR approach provides a complementary perspective to more established techniques on the hydrogen bonding, electrostatics, and dynamics of protein. In addition, it has the following six useful attributes. First, isotope labeling does not perturb molecular structure like large fluorescent or non-natural nitroxide spin labels. Second, it requires only micrograms of material, whereas NMR usually requires milligrams. Third, 2D IR spectroscopy may be applied to a broad range of systems, including membrane-bound, aggregated, and soluble proteins. Fourth, lipid bilayers can be used rather than micelles as some techniques require, which is especially important for conformationally flexible systems like ion channels. Fifth, 2D IR spectroscopy can be used to study protein dynamics and folding across all relevant time scales.[27−29] Finally, and perhaps most importantly, 2D IR spectra can be modeled from molecular dynamics simulations to provide a direct link between experiments and simulations.

The ability to calculate 2D IR spectra directly from molecular dynamics simulations is a particularly attractive feature, because precise details about the structure can be tested by comparison to experiments. In principle, generating infrared spectra from molecular dynamics simulations just requires a simple Fourier transform of classical dipole time-correlation functions, but in practice such an approach is not accurate enough for quantitative comparison to experiments. However, in the past few years, mixed quantum-classical methods have been developed for obtaining highly accurate 1D and 2D IR spectra from line shape theory using information from molecular dynamics simulations.[24,25,30−34] There are a number of different methods, but the basic premise of them all is that for each step in a molecular dynamics trajectory, the structure is used to generate vibrational frequencies with an electrostatic map derived from high-level ab initio calculations of model systems, and then IR spectra are calculated using line shape theory. The comparison of experiment and theory in this Article is an important benchmark in the development of these semiempirical methods. The methodology is exciting because it provides a direct means of testing molecular dynamics simulations and for interpreting the experimental results on the basis of first principles.

In this Article, we use $^{13}C{=}^{18}O$ isotope labeling, 2D IR spectroscopy, and molecular dynamics simulations to probe the membrane-bound structure of the ovispirin peptide. Ovispirin is an 18-residue polypeptide that resembles the N-terminal domain of the antimicrobial peptide SMAP-29.[35,36] It is α-helical in aqueous buffer and when bound to a lipid bilayer.[37] According to solid-state NMR experiments that measure the angles of N−H bonds in macroscopically aligned bilayers, the helical axis of ovispirin lies parallel to the membrane surface.[38] However, the solid-state NMR measurements only provided angular measurements, and, thus, the depth at which ovispirin lies in the membrane bilayer is unknown. Its rotational orientation is also unverified, although a helix wheel diagram puts all of the charged amino acids on one side of the helix (Figure 2c), as is typical for amphipathic peptides that bind parallel to the surface of negatively charged membranes.[4,7,15,39] The equilibrium depth is an important parameter to know, because it is related to the mechanism of antimicrobial action.[40,41] By isotope labeling nearly every residue in ovispirin and measuring the corresponding 2D IR spectra, we have observed an oscillatory pattern in the inhomogeneous line widths that is consistent with peripheral binding of ovispirin to the membrane in an α-helical structure. To characterize the depth of ovispirin in the membrane, its residue-specific secondary structure, and to understand the structural and electrostatic origin for this line shape trend, we calculated the free energy profile of ovispirin as a function of membrane depth, which predicts that the peptide lies just below the membrane headgroups. Using this structure, we calculated the 2D IR line shapes, which agree well with experiment. These simulations point to the strength and disorder of the electrostatic forces surrounding the amide I probe as the most important

(16) Lim, M. H.; Hamm, P.; Hochstrasser, R. M. *Proc. Natl. Acad. Sci. U.S.A.* **1998**, *95*, 15315–15320.
(17) Rella, C. W.; Kwok, A.; Rector, K.; Hill, J. R.; Schwettman, H. A.; Dlott, D. D.; Fayer, M. D. *Phys. Rev. Lett.* **1996**, *77*, 1648–1651.
(18) Bandaria, J. N.; Dutta, S.; Hill, S. E.; Kohen, A.; Cheatum, C. M. *J. Am. Chem. Soc.* **2008**, *130*, 22–23.
(19) Mukherjee, P.; Krummel, A. T.; Fulmer, E. C.; Kass, I.; Arkin, I. T.; Zanni, M. T. *J. Chem. Phys.* **2004**, *120*, 10215–10224.
(20) Fang, C.; Hochstrasser, R. M. *J. Phys. Chem. B* **2005**, *109*, 18652–18663.
(21) Mukherjee, P.; Kass, I.; Arkin, I.; Zanni, M. T. *Proc. Natl. Acad. Sci. U.S.A.* **2006**, *103*, 8571–8571.
(22) Mukherjee, P.; Kass, I.; Arkin, I. T.; Zanni, M. T. *J. Phys. Chem. B* **2006**, *110*, 24740–24749.
(23) Kim, Y. S.; Liu, L.; Axelsen, P. H.; Hochstrasser, R. M. *Proc. Natl. Acad. Sci. U.S.A.* **2008**, *105*, 7720–7725.
(24) Lin, Y. S.; Shorb, J. M.; Mukherjee, P.; Zanni, M. T.; Skinner, J. L. *J. Phys. Chem. B* **2009**, *113*, 592–602.
(25) Manor, J.; Mukherjee, P.; Lin, Y. S.; Leonov, H.; Skinner, J. L.; Zanni, M. T.; Arkin, I. T. *Structure* **2009**, *17*, 247–254.
(26) Kim, Y. S.; Liu, L.; Axelsen, P. H.; Hochstrasser, R. M. *Proc. Natl. Acad. Sci. U.S.A.* **2009**, *106*, 17751–17756.
(27) Chung, H. S.; Ganim, Z.; Jones, K. C.; Tokmakoff, A. *Proc. Natl. Acad. Sci. U.S.A.* **2007**, *104*, 14237–14242.
(28) Hamm, P.; Helbing, J.; Bredenbeck, J. *Annu. Rev. Phys. Chem.* **2008**, *59*, 291–317.
(29) Shim, S.-H.; Gupta, R.; Ling, Y. L.; Strasfeld, D. B.; Raleigh, D. P.; Zanni, M. T. *Proc. Natl. Acad. Sci. U.S.A.* **2009**, *106*, 6614–6619.
(30) Schmidt, J. R.; Roberts, S. T.; Loparo, J. J.; Tokmakoff, A.; Fayer, M. D.; Skinner, J. L. *Chem. Phys.* **2007**, *341*, 143–157.
(31) Jansen, T. L. C.; Knoester, J. *Biophys. J.* **2008**, *94*, 1818–1825.
(32) Zhuang, W.; Hayashi, T.; Mukamel, S. *Angew. Chem., Int. Ed.* **2009**, *48*, 3750–3781.
(33) Mukamel, S.; Abramavicius, D.; Yang, L. J.; Zhuang, W.; Schweigert, I. V.; Voronine, D. V. *Acc. Chem. Res.* **2009**, *42*, 553–562.
(34) Jeon, J.; Yang, S.; Choi, J. H.; Cho, M. *Acc. Chem. Res.* **2009**, *42*, 1280–1289.
(35) Kalfa, V. C.; Jia, H. P.; Kunkle, R. A.; McCray, P. B.; Tack, B. F.; Brogden, K. A. *Antimicrob. Agents Chemother.* **2001**, *45*, 3256–3261.
(36) Bartlett, K. H.; McCray, P. B.; Thorne, P. S. *Int. J. Antimicrob. Agents* **2004**, *23*, 606–612.
(37) Sawai, M. V.; Waring, A. J.; Kearney, W. R.; McCray, P. B.; Forsyth, W. R.; Lehrer, R. I.; Tack, B. F. *Protein Eng.* **2002**, *15*, 225–232.
(38) Yamaguchi, S.; Huster, D.; Waring, A.; Lehrer, R. I.; Kearney, W.; Tack, B. F.; Hong, M. *Biophys. J.* **2001**, *81*, 2203–2214.
(39) Hristova, K.; White, S. H. *Biophys. J.* **1999**, *76*, A219–A219.
(40) Zemel, A.; Ben-Shaul, A.; May, S. *J. Phys. Chem. B* **2008**, *112*, 6988–6996.
(41) Almeida, P. F.; Pokorny, A. *Biochemistry* **2009**, *48*, 8083–8093.

factors that contribute the most to the observed line width trends. Thus, we find that 2D IR spectroscopy can be used to probe the locations of residues in membrane-bound peptides and proteins on the basis of their electrostatic environment.

Experimental Section

Ovispirin samples were produced by incorporating individually isotope labeled amino acids into the peptide sequence using standard FMOC peptide synthesis protocols. Peptides were purified and combined with 3:1 1-palmitoyl-2oleoyl-sn-glycero-3-phosphocholine (POPC)/1-palmitoyl-2-oleoyl-sn-glycero-3-phosphoglycerol (POPG) lipid vesicles in an aqueous phosphate buffer using H_2O as the solvent, such that the lipid to peptide ratio was at least 21:1. Measurements were performed in H_2O solvent so that arginine side-chain absorption does not interfere with the isotope labeled peaks. Excess bulk H_2O was removed with a nitrogen stream to reduce absorption at 1650 cm^{-1} by the water bend vibrational mode. The bilayers are still fully hydrated as monitored by the water stretching band at 3300 cm^{-1}. At ~1595 cm^{-1}, the optical density (OD) of the isotope label was about 0.05. At the frequency of the isotope label, the H_2O bend added an additional OD of 0.25, but because 2D IR scales as the transition dipole, $|\mu|^4$, whereas FTIR scales as $|\mu|^2$, the water does not appreciably contribute to the 2D IR spectrum. 2D IR spectra were collected using a mid-IR pulse shaper and a pump−probe beam geometry. Simulations of ovispirin in a POPC/POPG bilayer were performed with GROMACS using the GROMOS87 force field.[42] After a 100 ns equilibration, trajectories were calculated from production runs of 100 ns for nonmutated and 50 ns for mutated peptides. From the production runs, 2D IR spectra were calculated every 5 ns over a 2 ns window. At each 2 fs time step, the electrostatic field on the carbon and nitrogen atoms in the amide bond is calculated and converted to a frequency using a map, from which the 2D IR spectra are generated. Details of our methods are given in the Supporting Information.

Results and Discussion

Ovispirin has the sequence H_2N-KNLRR IIRKI IHIIK KYG-COOH. For 11 of the residues, we isotope labeled the naturally occurring amino acid (N, K, L, G, or I) using acid-catalyzed ^{18}O exchange on the amino acid followed by protection of the primary amine and side chain for standard FMOC peptide synthesis. For residues 4, 5, 8, and 12, a $^{13}C{=}^{18}O$ labeled glycine mutation was performed instead, because the side-chain groups of R and H are synthetically more difficult to protect. The 2D IR spectrum of each of the 15 peptides was measured after mixing with POPC/POPG lipid vesicles. Under our sample conditions, the peptides are monomeric, α-helical, and peripherally bound to the bilayers.

Shown in Figure 1a is a 2D IR spectrum collected with ovispirin labeled at R8G. As is typical for 2D IR spectra, each vibrational mode creates a pair of out-of-phase peaks along the diagonal and cross peaks between coupled modes. The diagonal peak pair at 1747 cm^{-1} is due to the ester stretch of the lipid headgroups, the pair at 1655 cm^{-1} is the unlabeled amide I band, and the pair at 1546 cm^{-1} is the amide II band. The $^{13}C{=}^{18}O$ labeled band that we are the most interested in lies in a largely transparent region of the spectrum at 1590 cm^{-1} between the unlabeled amide I and II bands (square box). There are cross peaks between many of these modes, including the isotope labeled peak and the unlabeled amide I, amide II, and lipid ester stretches. These cross peaks provide information on the secondary structure, protonation state, and vicinity to the lipid headgroups, all of which contain useful structural information, but are not the focus of this Article. For this study, we analyze the 2D line shapes of the isotope labeled mode at 1590 cm^{-1}.

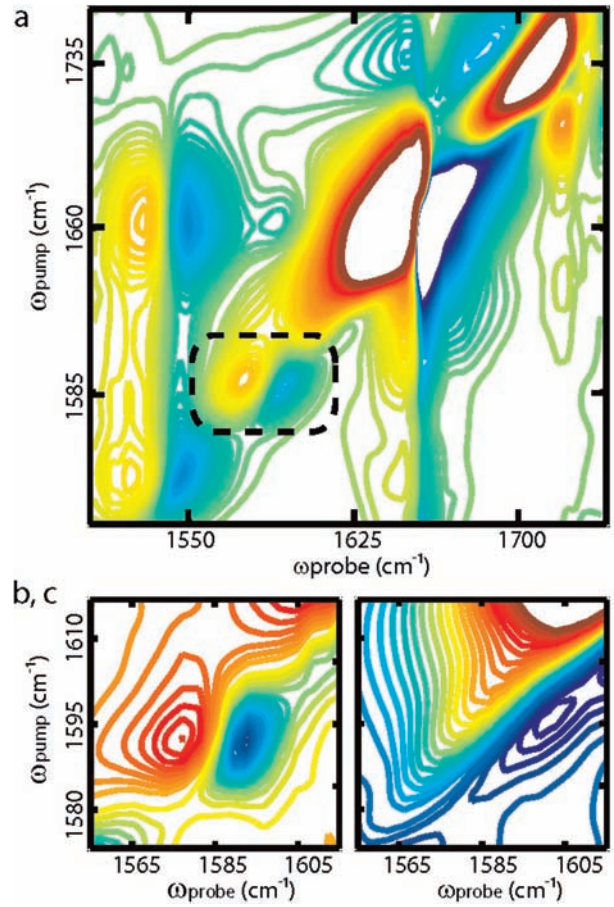

Figure 1. 2D IR spectra of $^{13}C{=}^{18}O$ labeled ovispirin. (a) 2D IR spectrum of ovispirin labeled at R8G, which spans the amide I through the lipid headgroup absorptions. The box highlights the labeled mode at ~1590 cm^{-1}. (b) 2D IR spectrum of just the region around the isotope label for I10 and (c) for K15. K15 is much more inhomogeneously broadened than I10, as indicated by its larger ellipticity along the diagonal.

Shown in Figure 1b and c are the 2D IR spectra of I10 and K15, respectively, for just the frequency range spanning the $^{13}C{=}^{18}O$ label. These 2D IR spectra have been collected using a mid-IR pulse shaper, which automatically generates absorptive line shapes and properly phased spectra. Phase cycling was used to remove scatter from the membranes and work in the rotating frame. There was no time delay between the mixing and probing pulses ($t_2 = 0$) so that the vibrational modes did not undergo spectra diffusion. We have published a recent review article on using pulse shaping to collect 2D IR spectra.[43] Because these spectra are line-narrowed, the width of the absorption along the antidiagonal gives the homogeneous line width, whereas the diagonal width is the total line width. Thus, the ellipticity of the peaks measures the amount of inhomogeneous broadening. For I10, the peaks are quite round, indicating that they are largely homogeneous. In contrast, the peaks for K15 are very elongated, indicating that they are extremely inhomogeneous. Thus, by simple visual inspection, it is clear that the amount of inhomogeneous character is very different between these two residues. The 2D IR spectra for all 15 residues are presented in the Supporting Information (Figure S1).

(42) Van Gusteren, W. F. B., H. J. C. *Groningen Molecular Simulation (GROMOS) Library Manual*; Biomos: Groningen, The Netherlands, 1987.

(43) Shim, S.-H.; Zanni, M. T. *Phys. Chem. Chem. Phys.* **2009**, *11*, 748–761.

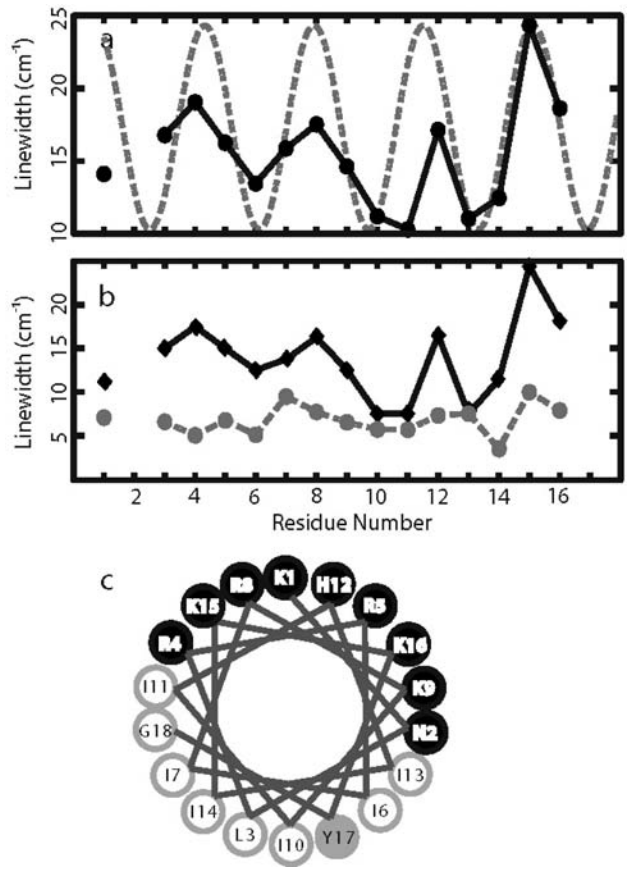

Figure 2. 2D IR line widths taken from Table S1. (a) Diagonal line widths for each labeled residue. (b) Inhomogeneous (solid) and homogeneous line widths (dashes). (c) Helical wheel diagram showing ovispirin amphipathy. Hydrophilic and hydrophobic residues are colored dark and light, respectively.

Isotope labeling with $^{13}C{=}^{18}O$ shifts the amide I band by about 60 cm^{-1} from the unlabeled peaks so that it is spectroscopically resolved, but the wings of the unlabeled amide I and the amide II bands still have non-negligible contributions in this frequency range. To remove these small but unwanted contributions, we fit the spectra using line shapes for the desired isotope labeled peaks, the amide II band, and the unlabeled amide I band. Crosspeak contributions to the diagonal line shapes are negligible and were ignored. The functional form of the line shapes is given in the Supporting Information and involves homogeneous and inhomogeneous contributions following Bloch dynamics. We have found in our previous studies that the amide I band of single isotopically labeled residues largely follows Bloch dynamics.[19,21,22] The fits to the spectra are shown in the Supporting Information (Figure S1), and in Table S1, we report the total diagonal, inhomogeneous, and homogeneous line width for each residue that we measured.

Of the parameters obtained from the fits, the most interesting are the diagonal line widths, which are plotted in Figure 2a. They display a periodic trend, with residues 4, 8, 12, and 15 at the crests of a sinusoidal wave that has troughs at residues 6, 11, and 13. The period of the oscillation matches the periodicity of an α-helix, which we ascertain by comparison to a sine wave with a period of 3.6 residues (dashed). Thus, the periodicity indicates that ovispirin is indeed an α-helix when bound to POPC/POPG membranes. Shown in Figure 2c is a helical wheel diagram of ovispirin. A comparison of the diagonal widths to the helical wheel diagram reveals that the residues with the broadest diagonal line widths (4, 8, 12, and 15) all fall on the same side of the helix whereas the residues with the narrowest diagonal line widths are located on the opposite side. There is a ∼140% difference in diagonal line width between the largest and narrowest diagonal line width in ovispirin (24.3 and 10.3 cm^{-1}, respectively). To ensure that the variations in line width are caused by membrane binding of monomers and not from interactions between peptides, we also measured the 2D IR spectra of three labeled peptides at one-half the peptide concentration. These dilution experiments produced negligible changes in line widths (see Supporting Information, S2) and confirm that ovispirin is bound to the membrane as monomers.

The trend observed in the diagonal line widths is almost entirely due to changes in inhomogeneity. The homogeneous and inhomogeneous line widths from Table S1 are plotted in Figure 2b. The homogeneous line widths vary by just a few wavenumbers and show no discernible correlation to the peptide structure. In comparison, the inhomogeneous line widths closely track the diagonal line widths. In our previous work on the transmembrane peptide bundles CD3ζ and M2, we also found that the homogeneous line widths are roughly invariant, as have other studies.[19–22,24,25] Thus, we conclude that the homogeneous line widths are largely intrinsic for peptides and proteins and that the relevant information for 2D IR structural studies comes primarily from differences in inhomogeneous line widths caused by variations in the environments of residues facing into the membrane versus those facing outward.

To understand the origin of the trends observed in the 2D IR data and to draw more detailed structural conclusions from the experiments, we turn to molecular dynamics simulations (details are given in the Supporting Information). Shown in Figure 3a is the free energy profile of ovispirin as a function of the peptide distance from the center of the membrane bilayer (also see the Supporting Information). We observed a free energy minimum at a depth of 17.5 Å from the center of the bilayer. A representative snapshot of the structure is shown in Figure 3b. At this depth, the peptide lies just below the headgroups, which is illustrated by the number density profiles in Figure 3c. It is also tilted and loses its helicity for a few amino acids near residue 14. This is illustrated in Figure 3d, which contains a plot of the average depth of each backbone carbonyl calculated over the course of the 100 ns trajectory. The carbonyl depth oscillates with a 3.6 residue period and is deeper at the N- than the C-terminus, which is a consequence of the α-helix being tilted in the bilayer. At residues 13 and 14, the helix unravels for one-half of the trajectory, which destroys the periodic trend at this point and indicates that the α-helical secondary structure is less stable in this region of the peptide.

To compare directly the molecular dynamics simulations with experiment, we generated ensemble-averaged (over the 100 ns trajectory) 2D IR line shapes for each residue in ovispirin. To calculate the spectra for the mutant peptides, independent trajectories were run for each, starting with the initial conformation of the natural peptide, performing the mutation, and then equilibrating the structure for 15 ns before the simulating the 2D IR spectra during the final production run. To convert the molecular dynamics simulation trajectories into 2D IR spectra, at each time step the projection of the electric field on the carbon and nitrogen atoms in the direction of the carbonyl bond was calculated, and an empirically derived map was used to determine the transition frequency.[24] Mixed quantum-classical line shape formalism was then used to convert the frequency

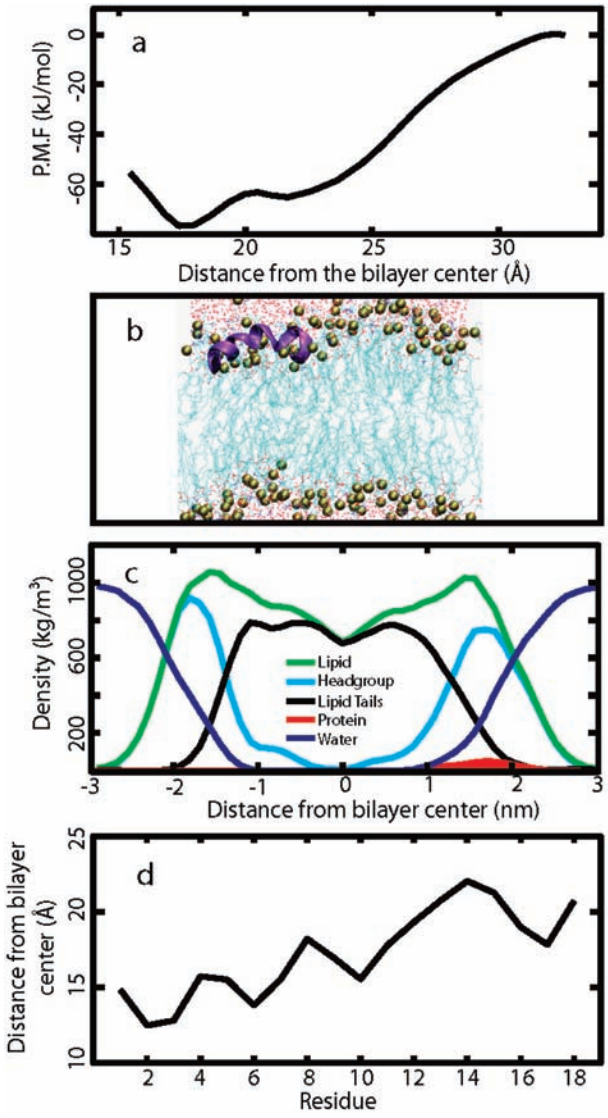

Figure 3. Results from molecular dynamics simulations. (a) Potential mean force (PMF) as a function of distance from the bilayer center. (b) Representative snapshot of structure at 17.5 Å from bilayer center. (c) Density profile of the various groups (as defined in the figure) along the bilayer normal. (d) Average depth of α-carbons in each residue over the course of the simulation trajectory.

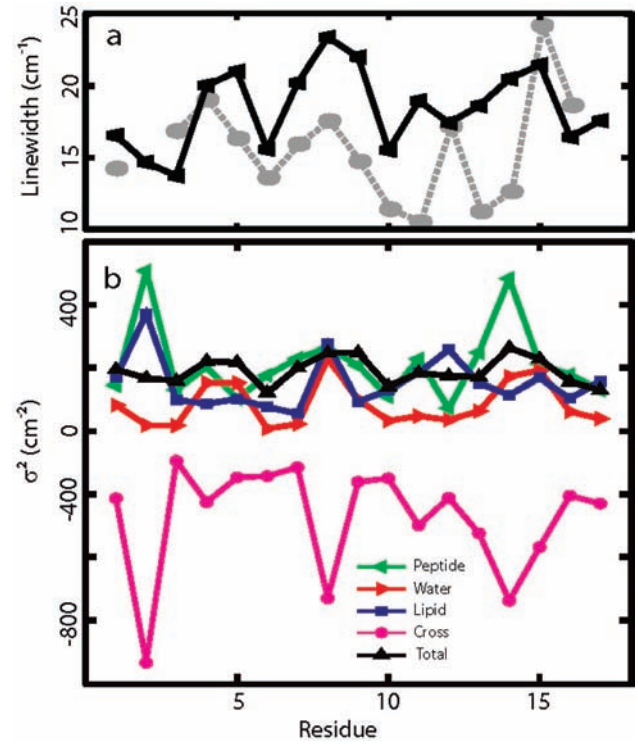

Figure 4. 2D IR data calculated from molecular dynamics simulation. (a) Diagonal line width of calculated amide I mode for each residue (solid black line) with experimental line widths (dashed gray line) reproduced from Figure 2a for comparison. (b) Contributions to the frequency variance for each residue.

trajectories into 2D IR spectra. Our methodology is described in detail in the Supporting Information.

The 2D IR diagonal line widths calculated from the molecular dynamics simulations are shown in Figure 4a. For residues that were mutated, the line width of the simulated mutant is given for that mutated residue, so that the experimental points are directly comparable to the experiment. These are seen to be in quite good agreement with the experimental line widths in Figure 2a. They also closely mimic the carbonyl depths in Figure 3d. The largest line width predicted by simulation is 23 cm^{-1}; the smallest is 13.7 cm^{-1}, which gives a dynamic range of about 80%. For residues 1−11, the simulations predict an oscillation in the line widths that scales about linearly with the carbonyl depth. The periodicity is lost beginning at residue 12, just before the position in which the peptide helicity breaks down (due to changes in H-bonding). This is most obvious for residue 14, which has conspicuously large frequency fluctuations for a residue that would be expected to face the bilayer interior if the peptide was a perfectly formed α-helix. To understand better the origin of these simulated line widths, we also calculated the variance of the frequency fluctuations (σ^2), which measures the distribution of frequency fluctuations, but does not include the dynamics that contribute to line width narrowing, and broke them down into their respective contributions from the peptide, water, and lipids, which are shown in Figure 4b (the ions make negligible contributions, which are not shown). Also shown is the total variance and the sum of the cross terms. The total variance closely tracks the diagonal line widths (Figure 4a), indicating that the fast frequency fluctuations that cause line narrowing and determine the homogeneous line width are about the same for all of the residues, as was observed in the experiments (Figure 2b). All three components (peptide, lipid, and water) contribute about equally to the frequency fluctuations of each residue, except for residues that reside on the bottom of the helix, which have smaller contributions from (largely absent) water. However, the observed infrared line widths cannot be straightforwardly decomposed into their individual components because their frequency fluctuations are correlated. The cross terms are a measure of their correlation, which are negative and nearly equal in magnitude to the individual contributions themselves. Thus, on average, the frequency fluctuations caused by one component are strongly offset from the others due to correlated structural motions.

The 2D IR measurements performed here provide a nearly instantaneous snapshot of the structural distribution of ovispirin and its environment. On the 1−2 ps time scale with which the amide I free induction decay lasts, very little motions occur. Water hydrogen-bond dynamics occur on this time scale as do high frequency backbone fluctuations, but little else. Thus, the 2D IR frequencies and line widths of ovispirin are a measure of the intrinsic structural disorder of the peptide and its

surrounding membrane environment. However, the line shapes do not reflect all types of structural disorder equally. We have found that the residues on the helix that face the interior of the membrane bilayer are much less inhomogeneously broadened than residues facing the headgroups and water, even though the lipid tails of bilayers are highly disordered.[44] Thus, disordered but nonpolar environments have little effect on the amide I line shape, because the amide I mode is mostly sensitive to electrostatic forces. In our previous work on the CD3ζ and M2 transmembrane peptide bundles that span the membrane, we observed narrower amide I line widths for residues in the center of the membrane than for residues near the membrane/water interface, which is consistent with our results here.[19,21,22,25] For ovispirin, a surface-bound peptide, the change in electrostatics across the region of the membrane at which ovispirin lies causes a 14 cm^{-1} change in the amide I line width, which is large enough to be easily quantified with 2D IR spectroscopy. Thus, we have now shown that 2D IR line shapes can be used to probe the three most common structural motifs of α-helical bound membrane peptides, which are transmembrane peptides, ion channels, and peripherally bound peptides.

The fact that the 2D IR line widths scale with the strength and disorder of the electrostatic environment provides an intuitive manner in which to interpret the experimental data; the more homogeneous is the 2D IR line shape, the deeper the backbone carbonyl lies in the bilayer. However, because the strongest contributions to the electrostatic forces are from atoms in the immediate vicinity of the vibrational mode (e.g., the first solvent shell), the exact line widths are determined by the atomic-level details of the peptide structure and bilayer environment. In this regard, the ability to simulate 2D IR spectra from molecular dynamics simulations provides a means to quantitatively investigate specific details about the peptide structure and its lipid environment. In fact, the comparison between simulation and experiment here leads to new insights about ovispirin structure and membrane binding. NMR studies indicate that ovispirin is an α-helix that lies parallel to the plane of the bilayer with the hydrophobic residues facing the interior, but these studies could not determine the depth of the peptide in the bilayer.[38] In our work, the simulated 2D line widths exhibit an oscillatory trend between residues 1−11 that has a period, phase, and amplitude that closely resembles the experiment. Thus, the secondary structure, the packing of the lipids and water around the peptide, as well as its average depth and rotational orientation in the bilayer are well-described by molecular dynamics. However, the simulations do not precisely match the experiments. It appears that the simulations and experiments differ on the tilt of the helix and the secondary structure of ovispirin near the C-terminus. The simulations place the peptide at an average depth of 17.5 Å from the bilayer center with a tilt that puts the N-terminal deeper in the bilayer than the C-terminal by about 4 Å. The overall depth of ovispirin predicted by our molecular dynamics simulations is reasonable because the depth is in agreement with neutron scattering experiments and fluorescent quenching studies on similar peptides.[4,5,7,9,14] However, the experimental 2D IR line widths narrow by about 5 cm^{-1} (on average) from residues 3 to 11, whereas the simulated line widths broaden about 5 cm^{-1} over these same residues. Thus, it appears that the simulations do not capture the proper tilt of ovispirin in the bilayer. Such a difference is not unexpected, because a 100 ns molecular dynamics simulation is not long enough to sample fully low-frequency structural modes like the tilt. There are, of course, also the inevitable questions about force-field accuracy. Regarding the structure of ovispirin at the C-terminus, the experiments exhibit a sinusoidal trend in line widths across the entire length of the peptide, suggesting continuous α-helical secondary structure for all measured residues. In comparison, the simulations predict a breakdown in helicity for residues 13−15 so that an oscillatory trend is not predicted for these residues. It is possible that the helix is kinked at this position, which could reconcile the experiment and simulations. We know from our work on the CD3ζ peptide that kinks in α-helices increase the inhomogeneous line width,[21,22] which may explain the abrupt increase in the measured line widths of residues 15 and 16. In fact, solid-state NMR experiments that measure the orientation of NH bonds in oriented bilayers also suggest there is a kink near the C-terminus. It is likely that the molecular dynamics trajectory is too short to fully sample the range of peptide conformations near residue 14. The presence of a kink could be tested, as could the helix tilt, with steered molecular dynamics simulations in which the 2D IR spectra are calculated for a peptide that is constrained to the structure inferred from the experiments. These are important issues for the antimicrobial action of ovispirin, because the peptide depth influences the curvature of the membrane[40,41] and its secondary structure degrades the integrity of the bilayer.[44]

Of course, the accuracy with which the molecular dynamics simulations can be converted into 2D IR spectra depends on the quality of the mixed quantum-classical method of calculating the line shapes. To calculate the frequency trajectories from the molecular dynamics simulations, we used a correlation map derived from calculations of a single peptide bond (*N*-methylacetamide) in water.[24] The map is expected to work well for small peptides in water, but not as well for hydrophobic environments for which it was not parametrized. Other maps are currently being developed. Even so, the parametrization is already very good, because we correctly predict the line widths to less than 5 cm^{-1} for all residues, and the variation in line width from one side of the helix to the other matches the experiment. The ability to convert molecular dynamics simulations into 1D or 2D IR spectra is very promising, because the conversion only requires simulations of a few hundred picoseconds. As a consequence, the problem reduces to generating the appropriate ensemble average of the structural distribution, but does not require unfeasibly long trajectories for the spectral calculation itself. Thus, infrared spectroscopy provides a direct comparison between simulations and experiment grounded on first principles that is not readily available for other spectroscopies.

The periodic trend in the 2D IR line widths is caused by the α-helical structure of ovispirin and the gradient of electrostatic forces that exist in bilayers. The interfacial region in which the bilayer changes from hydrophobic to hydrophilic is illustrated in the relative partial density plots of Figure 3c that are calculated from the molecular dynamics simulations. For this POPC/POPG bilayer composition, the bilayer half-thickness is about 30 Å, of which the headgroups span 10 Å. The water concentration transitions to the bulk over a distance of about 15 Å. At a depth of 17.5 Å, the peptide lies just below the headgroups so that one side of the helix is hydrated while the other resides in the hydrophobic interior of the bilayer. If the peptide resided in the very center of the bilayer or was only weakly bound to the membrane surface, then we would expect to see very small differences in line width because opposite

(44) Jaud, S.; Tobias, D. J.; Falke, J. J.; White, S. H. *Biophys. J.* **2007**, *92*, 517–524.

sides of the α-helix would have similar environments. Yet because the diameter of an α-helix (∼9 Å) is only slightly smaller than the width of the interfacial region, we expect that the amide I vibrational modes are sensitive to depth at all relevant positions in the bilayer. This conclusion is supported by our work on the CD3ζ and M2 peptide bundles, which showed continuous differences in line width across the bilayer interior.[19,21,22,25] Other secondary structures, such as β-hairpins, should exhibit unique line width trends as well. Moreover, because the 2D IR line widths are mostly determined by the local electrostatic environment of the amide I groups, it might be possible to enhance or suppress the line widths by adding reagents to the solvent, like is done in EPR or NMR paramagnetic relaxation experiments,[8,12,45] or by mutations that cause local changes in hydration. In fact, molecular dynamics simulations could be used to help design reagents and test the effect of possible mutations.

Along these lines, we have used molecular dynamics to ascertain the effect of the mutations on the structure of the peptide and changes in their environment. We calculated the α-carbon depth for each of the equilibrated mutant peptides and found that the backbone depth is unchanged from the native sequence (Figure S3a). We also looked at the effect of mutated side chains on hydration structure around the labeled backbone and found little or no difference in the standard deviation of hydrogen bonded water molecules. Although one can always argue that the molecular dynamics simulations are too short to determine the effects of the mutations on the global structure, the results are reasonable because the experimental trend we observe is consistent with the α-helical backbone of ovispirin. Thus, the specific nature of the side chains makes a smaller contribution to the line widths than does the depth or backbone in the bilayer.

Conclusion

This Article reports that the natural vibrational modes of membrane peptides can be exploited to study their structure and mode of binding. Our approach is complementary to other structural techniques for a variety of reasons, one of which is the ability to compare quantitatively 2D IR spectra to molecular dynamics simulations. Because of longer time scales and other factors, a direct comparison of molecular dynamics simulations to other spectroscopies can be problematic. However, the fast free induction decay time of vibrations makes calculation of infrared spectra easily tractable with simulations. For ovispirin, we found that the free energy minima predicted by simulations agrees well with the experiment, except for the tilt of the helix and the amount of α-helical content near the C-terminal end of the peptide. These results have implications for the antimicrobial mechanism of ovispirin in addition to providing a benchmark system for improving the conversion of molecular dynamics trajectories to infrared spectra. We think that this infrared approach will have important applications to systems that cannot tolerate spin or fluorescence labels, such as the interiors of ion channels or the active sites of enzymes, and in systems that cannot be studied using micelles. Of course, the 2D IR method is not limited to equilibrium studies but can be used to monitor changes in line widths in kinetically evolving systems as well, such as amyloid aggregation. In principle, equivalent line width information could be obtained with simple FTIR spectroscopy, because it appears for all systems studied so far that the homogeneous line width of amide I vibrational modes are largely invariant to peptide structure and environment. Thus, while 2D IR spectroscopy has many advantages over FTIR spectroscopy such as its ability to suppress background absorptions, the approach of isotope labeling and line width analysis could become a widely used tool because FTIR spectrometers are commonly available in many biophysics laboratories. Finally, we note that non-natural infrared probes, such as nitrile groups, are also being developed in an analogous manner.[46–49] Nitrile groups can perturb protein structures, but are much smaller than EPR or fluorescence labels. Moreover, they exhibit frequency shifts and line width changes in peptides bound to membranes.[46] Taken all together, site-specific natural and non-natural labeling, 2D IR spectroscopy, and molecular dynamics simulations are helping to develop infrared spectroscopy into a more quantitative structural tool.

Acknowledgment. Support for this research was provided by the NSF through a CRC grant (0832584) to M.T.Z. and J.L.S. This work was also supported by the National Science Foundation through the UW-MRSEC on Nanostructured Interfaces and Grant No. CBET-0755730 to J.J.d.P. We are also grateful to D. P. Raleigh for helpful discussions.

Supporting Information Available: More detailed methods, spectra for each isotope labeled peptide, and data tables. This material is available free of charge via the Internet at http://pubs.acs.org.

JA9101776

(45) Livshits, V. A.; Dzikovski, B. G.; Marsh, D. *J. Magn. Reson.* **2001**, *148*, 221–237.
(46) Mukherjee, S.; Chowdhury, P.; DeGrado, W. F.; Gai, F. *Langmuir* **2007**, *23*, 11174–11179.
(47) Suydam, I. T.; Snow, C. D.; Pande, V. S.; Boxer, S. G. *Science* **2006**, *313*, 200–204.
(48) Oh, K. I.; Choi, J. H.; Lee, J. H.; Han, J. B.; Lee, H.; Cho, M. *J. Chem. Phys.* **2008**, *128*, 154504–154510.
(49) Kozinski, M.; Garrett-Roe, S.; Hamm, P. *J. Phys. Chem. B* **2008**, *112*, 7645–7650.